

**PERFORMANCE IMPROVEMENT OF SPLIT SAVONIUS ROTOR BY CFD**

**NUR HAYATI BINTI HASSAN**

**UNIVERSITI TEKNIKAL MALAYSIA MELAKA**

**PERFORMANCE IMPROVEMENT OF SPLIT SAVONIUS ROTOR  
BY CFD**

**NUR HAYATI BINTI HASSAN**

**This report is submitted  
in fulfillment of the requirement for the degree of  
Bachelor of Mechanical Engineering (Thermal-Fluids)**

**Faculty of Mechanical Engineering**

**UNIVERSITI TEKNIKAL MALAYSIA MELAKA**

**MAY 2017**

## DECLARATION

I declare that this project report entitled Performance Improvement of Split Savonius Rotor by CFD is the result of my own work except as cited in references.

Signature : .....

Name : .....

Date : .....

## APPROVAL

I hereby declare that I have read this project report and in my opinion this report is sufficient in terms of scope and quality for the award of Bachelor of Mechanical Engineering (Thermal-Fluids)

Signature : .....

Name of Supervisor : .....

Date : .....

## **DEDICATION**

To my beloved husband, Mohd Anis bin Abd Rahman.

## ABSTRACT

Split Savonius wind turbine is a type of vertical axis wind turbine. Conventional Split Savonius wind turbine consists of two blades, advancing and returning. Advancing blade produces drag force from main flow while returning blade develops return force from opposite direction through a gap called overlap. Two types of torque are generated due to rotational motion of these blades against working fluid, positive and negative torque. Main objective of present study is to conduct a two dimensional numerical analysis between conventional Split Savonius rotor and new configurations in term of net positive torque and coefficient of performance (COP). Three new configurations are designed based on conventional Split Savonius rotor by keeping end plate diameter, overlap and aspect ratio constant. A validation study is performed by comparing torque obtained by numerical approach with torque obtained by experimental approach. Validated methodology is adopted to simulate new configurations. An improvement in COP ranging from 0.78% to 1.33% for different inlet velocities is achieved for new configuration Design 1. Other designs show negative improvement.

## **ABSTRAK**

*Turbin angin Split Savonius adalah sejenis turbin angin vertikal. Turbin angin Split Savonius yang asas terdiri daripada dua jenis bilah iaitu bilah mara dan bilah kembali. Bilah mara menghasilkan daya seret dari aliran utama manakala bilah kembali menghasilkan daya kembali dari arah bertentangan melalui jurang yang dikenali sebagai pertindihan. Dua jenis daya kilas dijana daripada pergerakan putaran antara bilah-bilah ini dan bendalir yang digunakan iaitu daya kilas positif dan negatif. Objektif utama kajian ini adalah untuk mengendalikan analisa numerik dua dimensi antara pemutar asas Split Savonius dan konfigurasi baru dari segi daya kilas positif bersih dan pekali prestasi. Tiga jenis konfigurasi baru direka berdasarkan pemutar asas Split Savonius dengan mengekalkan diameter plat, pertindihan dan nisbah aspek malar. Kajian pensahihan dilaksanakan dengan membandingkan nilai daya kilas yang diperolehi daripada kaedah numerik dengan nilai daya kilas yang diperolehi daripada kaedah eksperimentasi. Metodologi yang sah tersebut digunakan bagi mensimulasi konfigurasi baru. Peningkatan pekali prestasi antara nilai 0.78% sehingga 1.33% telah dicapai bagi halaju masuk yang berbeza-beza untuk konfigurasi 1. Konfigurasi-konfigurasi lain tidak menunjukkan sebarang peningkatan.*

## **ACKNOWLEDGEMENT**

Alhamdulillah. I would like to express my greatest appreciation towards my supervisor, Dr. Cheng See Yuan who I would not be able to complete this study without. Thank you for accepting me as your PSM's student and giving me the opportunity to learn so much from you. Thank you for constantly advising and guiding me throughout this study with patience.

I would like to thank other FKM lecturers for sharing their knowledge in respective area of study. I would also like to thank UTeM's CAE assistant engineer, Mr. Rizal for allowing me to use the facility and ensuring it is in the best condition.

I would like to thank my course mates for their contribution in this study. Last but not least I would like to express my gratitude towards my family for their endless support and encouragement.



## CONTENT

CHAPTER	CONTENT	PAGE
	<b>DECLARATION</b> .....	<b>ii</b>
	<b>APPROVAL</b> .....	<b>iii</b>
	<b>DEDICATION</b> .....	<b>iv</b>
	<b>ABSTRACT</b> .....	<b>v</b>
	<b>ABSTRAK</b> .....	<b>vi</b>
	<b>ACKNOWLEDGEMENT</b> .....	<b>vii</b>
	<b>LIST OF FIGURES</b> .....	<b>x</b>
	<b>LIST OF TABLES</b> .....	<b>xiii</b>
	<b>LIST OF ABBREVIATIONS</b> .....	<b>xiv</b>
	<b>LIST OF SYMBOLS</b> .....	<b>xv</b>
	<b>INTRODUCTION</b> .....	<b>1</b>
	1.1 BACKGROUND .....	1
	1.2 PROBLEM STATEMENT .....	3
	1.3 OBJECTIVE .....	4
	1.4 SCOPE OF PROJECT .....	4
	<b>LITERATURE REVIEW</b> .....	<b>5</b>
	2.1 ENERGY IN THE WIND .....	5
	2.2 WIND TURBINE .....	6
	2.3 OPTIMIZATION OF SAVONIUS WIND TURBINE .....	7
	2.3.1 BLADE DESIGN .....	7
	2.3.2 NUMBER OF BLADES.....	10
	2.3.3 END PLATE DESIGN .....	11
	2.3.4 NUMBER OF STAGES .....	12
	2.3.5 OVERLAP RATIO .....	12
	2.3.6 ASPECT RATIO .....	13
	2.4 COMPUTATIONAL FLUID DYNAMICS .....	13

<b>METHODOLOGY .....</b>	<b>15</b>
3.1 INTRODUCTION .....	15
3.2 GEOMETRY .....	17
3.3 MATHEMATICAL MODELLING .....	21
3.3.1 GOVERNING EQUATION .....	22
3.3.2 TURBULENCE MODELLING .....	23
3.3.3 MESHING .....	25
3.3.4 SETUP AND SOLUTION .....	33
3.3.5 SOLUTION CONVERGENCE .....	34
<b>RESULTS AND DISCUSSION .....</b>	<b>49</b>
4.1 VALIDATION STUDY .....	49
4.2 COMPARATIVE STUDY .....	50
<b>SUMMARY .....</b>	<b>75</b>
<b>REFERENCES .....</b>	<b>76</b>

## LIST OF FIGURES

Figure 1.1 Darrieus Wind Turbine. (Source: McAdam, 2016)	2
Figure 1.2 Conventional Savonius Wind Turbine. (Source: REUK.co.uk, Wenlong Tian, 2015)	2
Figure 1.3 Split Savonius Wind Turbine. (Source: Frederikus Wenehenubuna, Andy Saputraa, Hadi Sutanto, 2014)	3
Figure 2.1 Streamlines, primary and opposing torques. (Source: John Patrick Abraham, 2012)	7
Figure 2.2 40 Degree Twisted Blade. (Source: Abdul Qadir Versiani, 2015)	9
Figure 2.3 3D view of helical Savonius turbine. (Source: A. Reza Hassanzadeh, 2013)	9
Figure 2.4 Rotor configurations. (Source: J., 2007)	10
Figure 2.5 Applied boundary conditions. (Source: Sukanta Roy, 2013)	14
Figure 3.1 Methodology flow chart	16
Figure 3.2 Schematic of two-bladed conventional Split Savonius rotor. (Source: U.K Saha, 2008)	17
Figure 3.3 CAD drawing of computational domain for Conventional Split Savonius wind turbine	18
Figure 3.4 Schematic of Design 1	19
Figure 3.5 Schematic of Design 2	20
Figure 3.6 Schematic of Design 3	21
Figure 3.7 Triangular Meshing for Conventional Savonius	25
Figure 3.8 Transition between Stationary and Rotating Domains for Conventional Rotor	26
Figure 3.9 Prism Mesh Layers around Blade in Rotating Domain for Conventional Rotor	26
Figure 3.10 Triangular Meshing for Design 1	27
Figure 3.11 Transition between Stationary and Rotating Domains for Design 1	27
Figure 3.12 Prism Mesh Layers around Blade in Rotating Domain for Design 1	28

Figure 3.13 Triangular Meshing for Design 2	28
Figure 3.14 Transition between Stationary and Rotating Domains for Design 2	29
Figure 3.15 Prism Mesh Layers around Blade in Rotating Domain for Design 2	29
Figure 3.16 Triangular Meshing for Design 3	30
Figure 3.17 Transition between Stationary and Rotating Domains for Design 3	30
Figure 3.18 Prism Mesh Layers around Blade in Rotating Domain for Design 3	31
Figure 3.19 Mesh Metrics Spectrum. (Source: Ozen Engineering, 2014)	32
Figure 3.20 Monitors for Conventional rotor at $V = 6.0$ m/s (a) scaled residual (b) moment coefficient (c) drag coefficient (d) lift coefficient	37
Figure 3.21 Monitors for Conventional rotor at $V = 8.23$ m/s (a) scaled residual (b) moment coefficient (c) drag coefficient (d) lift coefficient	38
Figure 3.22 Monitors for Conventional rotor at $V = 10.17$ m/s (a) scaled residual (b) moment coefficient (c) drag coefficient (d) lift coefficient	39
Figure 3.23 Monitors for Design 1 rotor at $V = 6.0$ m/s (a) scaled residual (b) moment coefficient (c) drag coefficient (d) lift coefficient	40
Figure 3.24 Monitors for Design 1 rotor at $V = 8.23$ m/s (a) scaled residual (b) moment coefficient (c) drag coefficient (d) lift coefficient	41
Figure 3.25 Monitors for Design 1 rotor at $V = 10.17$ m/s (a) scaled residual (b) moment coefficient (c) drag coefficient (d) lift coefficient	42
Figure 3.26 Monitors for Design 2 rotor at $V = 6.0$ m/s (a) scaled residual (b) moment coefficient (c) drag coefficient (d) lift coefficient	43
Figure 3.27 Monitors for Design 2 rotor at $V = 8.23$ m/s (a) scaled residual (b) moment coefficient (c) drag coefficient (d) lift coefficient	44
Figure 3.28 Monitors for Design 2 rotor at $V = 10.17$ m/s (a) scaled residual (b) moment coefficient (c) drag coefficient (d) lift coefficient	45
Figure 3.29 Monitors for Design 3 rotor at $V = 6.0$ m/s (a) scaled residual (b) moment coefficient (c) drag coefficient (d) lift coefficient	46
Figure 3.30 Monitors for Design 3 rotor at $V = 8.23$ m/s (a) scaled residual (b) moment coefficient (c) drag coefficient (d) lift coefficient	47
Figure 3.31 Monitors for Design 3 rotor at $V = 10.17$ m/s (a) scaled residual (b) moment coefficient (c) drag coefficient (d) lift coefficient	48
Figure 4.1 Coefficient of moment against inlet velocity for conventional rotor, design 1, design 2 and design 3	51

Figure 4.2 Torque per height against inlet velocity for conventional rotor, design 1, design 2 and design 3	52
Figure 4.3 Coefficient of performance against inlet velocity for conventional rotor, design 1, design 2 and design 3	52
Figure 4.4 Variation of torque of conventional rotor with time value for $V = 6.0$ m/s	54
Figure 4.5 Variation of torque of conventional rotor with time value for $V = 8.23$ m/s	55
Figure 4.6 Variation of torque of conventional rotor with time value for $V = 10.17$ m/s	56
Figure 4.7 Variation of torque of Design 1 rotor with time value for $V = 6.0$ m/s	57
Figure 4.8 Variation of torque of Design 1 rotor with time value for $V = 8.23$ m/s	58
Figure 4.9 Variation of torque of Design 1 rotor with time value for $V = 10.17$ m/s	59
Figure 4.10 Variation of torque of Design 2 rotor with time value for $V = 6.0$ m/s	60
Figure 4.11 Variation of torque of Design 2 rotor with time value for $V = 8.23$ m/s	61
Figure 4.12 Variation of torque of Design 2 rotor with time value for $V = 10.17$ m/s	62
Figure 4.13 Variation of torque of Design 3 rotor with time value for $V = 6.0$ m/s	63
Figure 4.14 Variation of torque of Design 3 rotor with time value for $V = 8.23$ m/s	64
Figure 4.15 Variation of torque of Design 3 rotor with time value for $V = 10.17$ m/s	65
Figure 4.16 Velocity Distribution for $V = 6.0$ m/s (a) Conventional (b) Design 1 (c) Design 2 (d) Design 3	67
Figure 4.17 Velocity Distribution for $V = 8.23$ m/s (a) Conventional (b) Design 1 (c) Design 2 (d) Design 3	68
Figure 4.18 Velocity Distribution for $V = 10.17$ m/s (a) Conventional (b) Design 1 (c) Design 2 (d) Design 3	69
Figure 4.19 Pressure Distribution for $V = 6.0$ m/s (a) Conventional (b) Design 1 (c) Design 2 (d) Design 3	70
Figure 4.20 Pressure Distribution for $V = 8.23$ m/s (a) Conventional (b) Design 1 (c) Design 2 (d) Design 3	71
Figure 4.21 Pressure Distribution for $V = 10.17$ m/s (a) Conventional (b) Design 1 (c) Design 2 (d) Design 3	72

## LIST OF TABLES

Table 1 Conventional Split Savonius Dimensions (Source: U.K Saha, 2008)	18
Table 2 Design 1 Dimensions	19
Table 3 Design 2 Dimensions	20
Table 4 Design 3 Dimensions	21
Table 5 Variation of Reynolds Number and Turbulence Intensity. (Source: U.K Saha, 2008)	23
Table 6 Estimated values of turbulent kinetic energy and turbulent dissipation rate. (Source: U.K Saha, 2008)	24
Table 7 Details of specific dissipation rate and turbulent viscosity ratio. (Source: U.K Saha, 2008)	24
Table 8 Total Number of Elements and Nodes	31
Table 9 Mesh quality metrics	31
Table 10 Percentage difference between torque CFD and torque U.K Saha et al.	50

## LIST OF ABBREVIATIONS

BC	Before Century
HAWT	Horizontal Axis Wind Turbine
VAWT	Vertical Axis Wind Turbine
CFD	Computational Fluid Dynamics
CAD	Computer Aided Drawing
2D	Two Dimensional
3D	Three Dimensional
RANS	Reynolds Average Navier Stokes
LES	Large Eddy Simulation
DNS	Direct Numerical Simulation
PDE	Partial Differential Equation
ASM	Algebraic Stress Model
RSM	Reynolds Stress Model
TBS	Tandem Blade Savonius
TSR	Tip Speed Ratio
RPM	Rotational Per Minute

## LIST OF SYMBOLS

$COP$	Power Coefficient/ Coefficient of Performance
$P_s$	Shaft Power/ Mechanical Power
$P$	Power Available in The Wind
$T$	Torque
$\Omega$	Angular Velocity/ Rotational Velocity
$\rho$	Density
$A$	Area
$V$	Velocity/ Speed
$D_f$	Diameter of End Plate
$D$	Diameter of Rotor
$D$	Diameter of Chord
$T$	Thickness of Chord
$E$	Overlap
$e'$	Second Overlap
$N$	Frequency of Rotation (rpm)
$\Lambda$	Tip Speed Ratio



# CHAPTER 1

## INTRODUCTION

### 1.1 BACKGROUND

The Sun radiates  $1.74 \times 10^{17}$  W energy to the Earth per hour and approximately 2% of this energy is converted into wind energy (Energy and Environment, 2016). Wind has been used as a source of energy as early as 5000 BC when wind energy is used to propel boats along Nile River (Wind Energy Foundation, 2016). By the end of 2015, 432.9GW wind power capacity has been installed globally led by Germany and United States of America (Global Wind Energy Council, 2016). This improvement has been possible with the use of wind turbine technology. Wind turbine is used to generate electricity by converting kinetic energy of the wind into mechanical energy which is used to turn the rotor and power up the generator, thus, generating electricity.

There are two types of wind turbine; horizontal axis wind turbine (HAWT) and vertical axis wind turbine (VAWT). These wind turbines can operate on either lift force, drag force or the combination of both. HAWT dominates the wind industry due to its efficiency compared to VAWT (Vertical Axis Wind Turbines vs Horizontal Axis Wind Turbines, 2009). HAWT is capable of achieving efficiency up to 50% whilst VAWT is only able to achieve efficiency approximately 15% (John Patrick Abraham, 2012). However, there are two types of VAWT which have the potential of being developed; Savonius wind turbine and Darrieus wind turbine (Figure 1.1) (Barnard, 2014). Conventional Savonius wind turbine (Figure 1.2) operates on drag force whereas Split Savonius wind turbine (Figure 1.3) operates on the combination of lift and drag forces (Fluid Mechanics: Fundamentals and Applications, 2010). Savonius wind turbine has low

efficiency due to lack of body force and surface force (Bagus Wahyudi, Sudjito Soeparmanb, H W M Hoeijmakersc, 2014). However, Savonius wind turbine is built due to its uncomplicated and low cost construction (Bagus Wahyudi, Sudjito Soeparmanb, H W M Hoeijmakersc, 2014) (Abdul Qadir Versiani, 2015). It is a slow rotating machine with higher torque compared to Darrieus wind turbine. Savonius rotor is not affected by the direction of wind thus suitable for non-uniform wind areas (Bagus Wahyudi, Sudjito Soeparmanb, H W M Hoeijmakersc, 2014) (Abdul Qadir Versiani, 2015). It is normally used for small water pumping applications.



Figure 1.1 Darrieus Wind Turbine. (Source: McAdam, 2016)

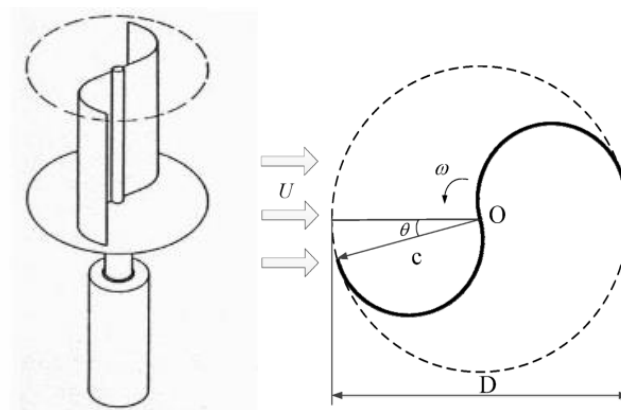


Figure 1.2 Conventional Savonius Wind Turbine. (Source: REUK.co.uk, Wenlong Tian, 2015)

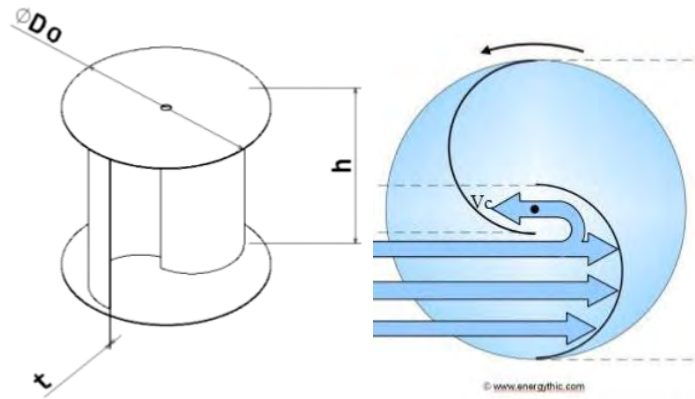


Figure 1.3 Split Savonius Wind Turbine. (Source: Frederikus Wenehenubuna, Andy Saputraa, Hadi Sutanto, 2014)

Basic Split Savonius wind turbine consists of two blades; advance blade and return blade. Advance blade produces drag force from main flow whereas return blade develops return force from opposite direction through a gap between blades called overlap. Overlap serves as an entry of outflow from advance blade to return blade. Overlap is the main difference between Conventional Savonius wind turbine and Split Savonius wind turbine (Bagus Wahyudi, Sudjito Soeparmanb, H W M Hoeijmakersc, 2014). There are few modification done to improve Split Savonius rotor in previous researches such as number of blades, blades twist angle, number of stages, overlap ratio, aspect ratio and end plates presence.

## 1.2 PROBLEM STATEMENT

Savonius wind turbine is a type of vertical axis wind turbine. Vertical axis wind turbine is known for its low efficiency compared to horizontal axis wind turbine. However, Savonius wind turbine possesses few advantages over horizontal axis wind turbine. Savonius wind turbine is used in non-uniform wind areas due to its independency towards direction of wind flow. It has low angular velocity compared to horizontal axis wind turbine but it is capable of generating higher torque. Therefore, in this study, rotor modification will be made to conventional Split Savonius rotor to increase its torque.

### **1.3 OBJECTIVE**

The research objective is:

1. To conduct a two dimensional comparative study between conventional Split Savonius rotor and new configured Split Savonius rotors by performing CFD analysis.

### **1.4 SCOPE OF PROJECT**

The scopes of research are:

1. Wind velocities used are 6.0, 8.23, and 10.17 m/s.
2. Modification is made to conventional Split Savonius rotor by changing the rotor shape to obtain higher torque.
3. Three new rotor configurations are drawn by using commercial software, ANSYS DesignModeler.
4. CFD simulation is performed by using commercial CFD software, ANSYS Fluent to study moment coefficient at the blades.
5. Torque and coefficient of performance are calculated by using these values.

## CHAPTER 2

### LITERATURE REVIEW

#### 2.1 ENERGY IN THE WIND

According to Albert Betz in 1919, any wind turbine regardless the design, is only capable of converting not more than 59.3% of wind kinetic energy into mechanical energy. Betz limit is also known as the theoretical maximum power efficiency of wind turbines. Power efficiency of wind turbine can be measured by using power coefficient equation, *COP*. *COP* is the ratio between mechanical power and power available in the wind.

$$COP = \frac{P_s}{P} \quad (2.1)$$

Where  $P_s$  , is the mechanical power and  $P$  is the power available in the wind. Mechanical power of wind turbine can be calculated by using equation (2.2).

$$P_s = T\omega \quad (2.2)$$

Where  $T$  is the mechanical torque (Nm) and  $\omega$  is the angular speed (rad/s). In the present study, brake torque is considered as mechanical torque for above equation. Angular speed can be calculated from equation (2.3).

$$\omega = \frac{2\pi N}{60} \quad (2.3)$$

Where  $N$  is the frequency of rotation for the rotor, (rpm).

Power available in the wind can be calculated by using equation (2.4).

$$P = \frac{1}{2}\rho AV^3 \quad (2.4)$$

Where  $\rho$  is the air density ( $\text{kg}/\text{m}^3$ ),  $A$  is the projected area of the rotor ( $\text{m}^2$ ) and  $V$  is the wind speed ( $\text{m}/\text{s}$ ).

## 2.2 WIND TURBINE

Bagus wahyudi et al. in his study states that Savonius wind turbine is a pure drag type wind turbine which highly influenced by density, blade sweep area and fluid velocity (Bagus Wahyudi, Sudjito Soeparmanb, H W M Hoeijmakersc, 2014). However, according to Abdullah Al-Faruk et al., it is observed that at low angle of attack, lift force contributes to the overall torque generation which then concluded Savonius wind turbine is a combination of drag and lift forces type of wind turbine (Abdullah Al-Faruk, 2016). As mentioned earlier VAWT has lower efficiency compared to HAWT. Regardless its low efficiency, VAWT is used due to several advantages. VAWT is smaller than HAWT thus requires smaller footprint compared to HAWT. Due to this advantage, some of VAWT application involves other building in which VAWT is mounted to such as cellular communication tower (John Patrick Abraham, 2012). VAWT does not need control system to search for wind direction as it is able to rotate regardless the flow direction. VAWT is able to start rotate at lower wind speed compared to HAWT thus it is suitable to be used for power generation at lower wind speed area. VAWT rotates slower than HAWT resulting in higher mechanical power compared to HAWT.

Figure 2.1 shows the airflow around Savonius rotor. In this figure, rotor is rotated clockwise. Air flow patterns are indicated by streamlines shown. As the inlet is located at bottom side of the figure, the flow is directed upward. Two torques generated by the flow; primary and opposing. Primary torque caused rotation in the direction of wind flow whilst opposing torque caused rotation to slow down. Therefore, in order to improve the rotor, primary torque must be higher than opposing torque.

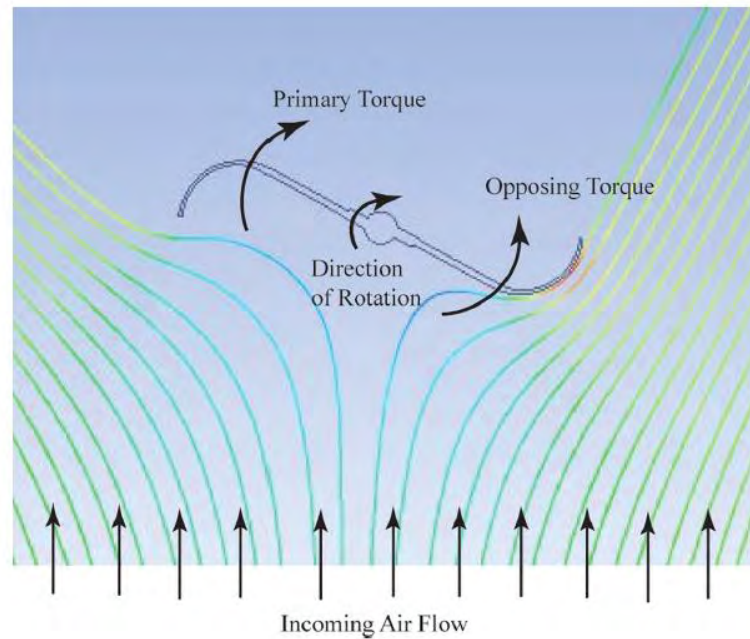


Figure 2.1 Streamlines, primary and opposing torques. (Source: John Patrick Abraham, 2012)

## 2.3 OPTIMIZATION OF SAVONIUS WIND TURBINE

Number of researches has been conducted to increase the efficiency of Savonius wind turbine. Mohammed Hadi Ali states that performance of Savonius wind turbine is related to these three principles; speed of blade tip is directly proportional to speed of the wind, maximum torque is proportional to the speed of wind squared and maximum power is proportional to the speed of wind cubed (Ali, 2013). Optimization of Savonius wind turbine is measured by using *COP* equation. Thus, researchers normally compared their new configurations with conventional torque which is then used to calculate *COP*.

### 2.3.1 BLADE DESIGN

Bagus Wahyudi et al. in his study designed a new configuration of blades by adding tandem blades and deflectors to the rotor (Bagus Wahyudi, Sudjito Soeparmanb, H W M Hoeijmakersc, 2014). Tandem blades are used to increase the projected area of the rotor which will improve the surface force thus, increase the force acting on return blade

and improve balancing of the couple forces. Previously, three models with different tandem blades configuration were simulated by CFD; Overlap TBS, Symmetrically TBS and Convergent TBS (B Wahyudi, 2013). By using maximum pressure gap between upstream and downstream equation, it is determined that Convergent TBS is capable of generating more power compared to the others. Water is used as working fluid in this study to increase the fluid momentum force acting on the blade. Response surface method and CFD show the variation in velocity and pressure near blades region. Pressure gap occurs across the rotor from upstream to downstream area indicate that power extracted by the rotor is causing it to rotate. Static pressure on convex side of both blades is lower than those on concave side due to high water velocity flowing over the convex side which produce torque to rotate the blades. Drag force acting on the return blade is increased due to compartment gap narrowing in tandem blades adjacent to the axis which increase pressure dynamics on the concave blades. It is observed that with the use of both deflector and tandem blade, velocity ratio on narrow gap and torque produced by drag force on return blade are improved compared to the configuration with tandem blades alone. Deflector caused positive static moment at any tip diameter for both angle deflector designs; radial and tangential whilst configuration without deflector shows the presence of negative values in some range.

Abdul Qadir Versiani et al. claimed in his study that twisted blade has lower negative projected area compared to conventional blade (Abdul Qadir Versiani, 2015). Twisted design caused the air flow to be swept inward and outward, creating a couple which ensure smooth rotation with higher rotational velocity and torque. An increase in velocity drop is shown from the inlet to the outlet via static and rotational analysis whilst static pressure contour shows that static pressure decreases from upstream to downstream area of the rotor which produces drag force and torque for the rotor. It is proven in his study that the optimum twisted angle is  $40^\circ$  as shown in Figure 2.2 where maximum velocity drop across the blade is achieved. It shows that most kinetic energy of the wind is successfully converted into mechanical energy. A study on twisted Savonius rotor is also performed by A. Reza Hassanzadeh et al. to study the comparison between conventional and Helical Savonius Marine Current Turbine (A. Reza Hassanzadeh, 2013). This study is using water as working fluid. Helical is chosen because twisted rotor has better self-start ability. It rotates smoothly but with high RPM at low flow velocity. Twisted rotor also has higher average power output and operates steadily. CFD is used to simulate helical rotor as